The final publication is available at

http://doi.org/10.1109/TED.2016.2614370

Additional Information

Analysis of Multipactor RF Breakdown in a Waveguide Containing a Transversely Magnetized Ferrite

D. González-Iglesias, Á. Gómez, B. Gimeno, *Member, IEEE*, Ó. Fernández, A. Vegas, *Member, IEEE*,
F. Casas, S. Anza, C. Vicente, J. Gil, R. Mata, I. Montero,
V. E. Boria, *Senior Member, IEEE*, D. Raboso

Abstract—In this paper, the multipactor RF breakdown in a parallel-plate waveguide partially filled with a ferrite slab magnetized normal to the metallic plates is studied. An external magnetic field is applied along the vertical direction between the plates in order to magnetize the ferrite. Numerical simulations using an in-house 3D code are carried out to obtain the multipactor RF voltage threshold in this kind of structures. The presented results show that the multipactor RF voltage threshold at certain frequencies becomes considerably lower than for the corresponding classical metallic parallel-plate waveguide with the same vacuum gap.

Index Terms—Multipactor effect, RF breakdown, parallel-plate waveguide, ferrite devices, magnetic field.

I. INTRODUCTION

Multipactor discharge is an undesired phenomenon that takes place on devices operating under vacuum conditions and high-power radio frequency (RF) electromagnetic fields [1], [2]. When certain conditions arise, free electrons in the device are driven by the RF electric field towards the walls. If the kinetic energy of the impacting electrons is high enough, secondary electrons may be released from the surface. As a consequence, a chain reaction leading to an exponential growth of the electron population inside the component is started. The onset of the multipactor discharge degrades the device performance by several negative effects, such as increasing the signal noise and reflected power, heating up the device walls, outgassing, detuning of resonant cavities, vacuum window failure, and even resulting in the total destruction of the

D. González-Iglesias, B. Gimeno and R. Mata are with Depto. Física Aplicada-ICMUV, Universidad de Valencia, Spain (email: daniel.gonzalez-iglesias@uv.es; benito.gimeno@uv.es; rafael.mata@uv.es)

Ó. Fernández, Á. Gómez and A. Vegas are with Depto. Ingeniería de Comunicaciones, Universidad de Cantabria, Spain (email: oscar.fernandez@unican.es; alvaro.gomez@unican.es; angel.vegas@unican.es)

F. Casas is with Instituto Universitario de Matemáticas y Aplicaciones (IMAC), Universidad Jaume I, Castellón, Spain (email: casas@uji.es)

S. Anza, C. Vicente and J. Gil are with AURORASAT, Valencia, Spain (email: sergio.anza@aurorasat.es; carlos.vicente@aurorasat.es; jordi.gil@aurorasat.es)

I. Montero is with Instituto de Ciencia de Materiales de Madrid, CSIC, Madrid, Spain (email: imontero@icmm.csic.es)

V. E. Boria is with Depto. Comunicaciones-iTEAM, Universidad Politécnica de Valencia, Spain (email: vboria@dcom.upv.es)

D. Raboso is with European Space Agency, ESA/ESTEC, The Netherlands (email: david.raboso@esa.int)

component. Due to that, multipactor phenomenon is revealed as a crucial limitation in the maximum RF power handling. Multipactor occurs in different environments such as passive components of satellite communication payloads, particle accelerators, and klystrons.

Special attention must be paid to multipactor in satellite components, where replacement of damaged devices is not possible. Therefore, in order to ensure that the RF component will not suffer this undesirable phenomenon during operation, it is extremely important to take into account this effect in the design process. In fact, restrictive specifications have been imposed by the space agencies about this issue [3].

Multipactor has been extensively analyzed in the case of metallic surfaces so far [4]-[6]. Recently, some studies have focused their attention to the case wherein dielectric surfaces are involved [7]-[9]. However, very little literature about multipactor effect in devices containing ferrites can be found [10], [11]. Ferrites are ferromagnetic materials which exhibit magnetic anisotropy when are brought under a DC magnetic bias field. When an external DC magnetic field is applied multipactor discharge can be either suppressed [12] or enhanced [13], depending on the specific magnitude and direction of the external field. The induced anisotropy in the ferrite has been used to produce a wide range of RF passive devices such as circulators, isolators and phase shifters [14]-[17]. Until now, the high power handling of this kind of components can only be analyzed by rough approximations whose validity is not clear.

The main aim of this paper is the study of the multipactor effect in an ideal uniform parallel-plate waveguide (as shown in Fig. 1) of infinite length along the x and z axis, z being the propagation direction of the electromagnetic wave, thus resulting an electromagnetic field which does not depend on the x-coordinate. Transmission of the fundamental TEM like mode is considered in this analysis. The waveguide contains a lossless ferrite slab which is magnetized along the direction perpendicular to the metallic walls, i.e., $\vec{H}_0 = H_0\,\hat{y}$. When the ferrite is saturation magnetized, it can be electromagnetically characterized by the constitutive relations $\vec{D} = \varepsilon\vec{E}$ and $\vec{B} = [\mu]\vec{H}$, wherein ε is the dielectric permitivitty and $[\mu]$ is the Polder's tensor corresponding to the aforementioned magnetization (eq. 9.27 of [14]). The effective field H_{ef} which magnetizes the ferrite is $H_{ef} = H_0 - M_s$ (see [14]), where M_s
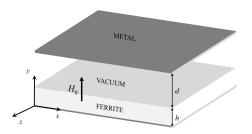
Fig. 1. Parallel-plate waveguide (considered to be infinite along the x and z axis, z being the propagation direction of the electromagnetic wave) partially loaded with a ferrite slab magnetized along the waveguide gap direction by a static magnetic field $\vec{H}_0$.

is the saturation magnetization. There is a gyromagnetic resonance of the ferrite at the Larmor frequency $\omega_0 = \gamma \mu_0 H_{ef}$, where μ_0 is the free space permeability, and $\gamma = e/m$ is the gyromagnetic ratio of the electron ($-e$ and m are the electron charge and electron mass at rest, respectively).

In a previous authors' work [11], which at first glance could be seen similar to the current one, the external magnetization field was oriented parallel to the ferrite slab. Since the magnetic permeability of the ferrite is anisotropic and depends on the bias magnetic field H_0 direction, the RF behavior of the ferrite in both cases is completely different. Moreover, the effect on the electron orbits due to changing the direction of the external magnetic field employed to magnetize the ferrite is crucial. Therefore, the present analysis is not only a straightforward extension of the previous one, and it is worthy of being studied.

This paper is structured as follows. First, in Section II, it is described both the multipactor algorithm and the method employed to compute the RF electromagnetic fields in such ferrite loaded waveguide. Next, Section III presents and analyzes the results of the multipactor simulations. Finally, the main conclusions of our study are summarized in Section IV.

II. THEORY

A. Multipactor Algorithm

The simulation code developed for the study of the multipactor is based on the single effective electron model [4]. This method consists of tracking the individual trajectories of a set of effective electrons. Each effective electron has associated a cumulative electron population that takes into account the emission or absorption of secondary electrons by the device walls. This is done by computing the value of the Secondary Electron Yield (SEY) function (δ) at each impact, which depends on the electron kinetic energy and impacting angle [18], [19]. After the impact, the colliding effective electron is launched back to the waveguide with random velocity given by a Maxwellian distribution with a mean certain kinetic energy (3 eV in our simulations). The velocity angle follows the cosine law distribution [20]. When the software has run for a predefined number of RF periods, the code stops and the time evolution of the total electronic population is shown.

The individual trajectories of the effective electrons are computed by solving numerically their non-relativistic equations of motion derived from the Lorentz Force. The total

electromagnetic field experienced by the electron is the superposition of the RF electric E_{RF} and magnetic B_{RF} fields, the electric field due to the space charge effect E_{sc}, the dc electric field appearing because of the charging of the ferrite surface E_{dc}, and the external magnetic field H_0 employed to magnetize the ferrite. Both E_{sc} and E_{dc} have been computed following the procedure reported in [7].

For the numerical integration of the differential equations of the electron trajectories we use a conveniently modified velocity-Verlet method. This particular scheme has very favorable properties concerning the error propagation in time, both in the energy and the position and velocity. We choose the time step size so that the relative error in position and in energy is less than 1% after a time of 200 RF periods.

B. RF Electromagnetic Field Computation

The RF electromagnetic field inside the structure under study has been obtained with the aid of the Coupled Mode Method (CMM). This well-known numerical method, formulated in the frequency domain, has been widely and successfully used in the analysis of the electromagnetic wave propagation inside uniform waveguides that contain any isotropic, anisotropic or complex material [21]-[23].

In few words, the Coupled Mode Method is a Method of Moments which consists on expanding the electromagnetic field components inside the structure under analysis in terms of a set of base functions previously defined [21]. In many cases these base functions correspond to the electric or magnetic field components of the TE and TM modes of the empty waveguide. Therefore, they are called basis modes. According to this idea, any component of the electromagnetic field of the structure under test can be expressed as a linear combination of the basis modes.

Once the electromagnetic fields inside the waveguide are obtained, the calculation of the equivalent voltage V_0 is done by integrating the vertical RF electric field along the vacuum gap.

III. SIMULATIONS

In order to compute the multipactor RF voltage threshold for the parallel-plate ferrite loaded waveguide shown in Fig. 1, numerical simulations have been performed. For all the considered cases, the ferrite thickness h and the vacuum gap d have been selected to match with the height of a WR-90 rectangular waveguide, i.e. $b = d + h = 10.16$ mm. The saturation magnetization of the ferrite is $4\pi M_s = 1806$ G, its relative dielectric permittivity $\varepsilon_r = 15$, and its SEY parameters are: first crossover energy for SEY coefficient equal to unity, $W_1 = 19$ eV, maximum SEY coefficient $\delta_{max} = 2.88$, and impact kinetic energy for δ_{max}, $W_{max} = 289$ eV [24]. For simplicity, the same SEY parameters are selected for the top metallic wall. The external magnetic field employed to magnetize the ferrite is $H_0 = 3000$ Oe. Consequently, the effective biasing field inside the ferrite is $H_{ef} = 1194$ Oe. The considered fields are those corresponding to the fundamental mode of the ferrite loaded waveguide (i.e., $l = 1$). For all calculations of the electromagnetic field components with the
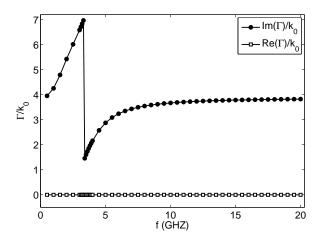
Fig. 2. Real and imaginary parts of the propagation factor for the fundamental mode of a ferrite loaded waveguide (with $d = 1$ mm) as a function of the RF frequency. Note that gyromagnetic resonance, given by Larmor frequency, occurs at 3.34 GHz.
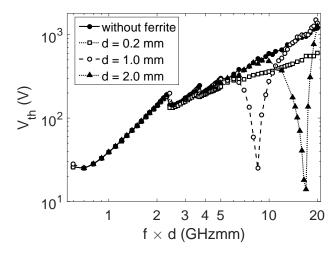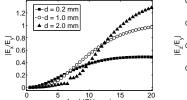

Fig. 3. Multipactor RF voltage threshold as a function of the frequency gap. Results are presented for parallel-plate ferrite loaded waveguides with different gap lengths and ferrite thicknesses (but maintaining the height of a WR-90 waveguide); and also for a metallic parallel-plate waveguide ("without ferrite").

Coupled Mode Method, a total number of 75 TE and 75 TM basis modes are used. These basis modes have been included by increasing their cut-off frequencies.

We are interested in analyzing the effect of the variation of the ferrite thickness and the vacuum gap length in the multipactor RF voltage threshold. First, for the fundamental mode, the propagation factor dependence with frequency it is obtained, as shown in Fig. 2. It can be observed that the real part of the propagation factor is zero within the plotted frequency range, which corresponds to a propagative mode.

In Fig. 3 the variation of the multipactor RF voltage threshold as a function of the frequency gap value (i.e., the multipactor susceptibility chart) is shown for several ferrite loaded parallel-plate waveguides. Note that for each curve the gap remains fixed. Moreover, the results for a classical metallic parallel-plate waveguide with no ferrite slab, a gap of $d = 0.2$ mm and $H_0 = 0$ (henceforth referred as without ferrite case) has been included for comparison purpose. Remember that according to the well-known multipactor theory [2] for a classical metallic parallel-plate waveguide, the multipactor phenomenon depends only on the frequency gap product and, as a consequence, the same multipactor RF voltage threshold curve would be obtained for metallic parallel-plate waveguides with other gaps while maintaining the same frequency gap range. From the results (recall Fig. 3) it is noticed that there is considerable difference between the multipactor RF voltage threshold of the ferrite loaded waveguides and the corresponding to the without ferrite case. It is found that this discrepancy increases with the gap value. In fact, the maximum difference in the multipactor RF voltage threshold between the $d = 0.2$ mm waveguide and the without ferrite case is of 6.5 dB, whilst in the $d = 1$ mm and $d = 2$ mm the difference becomes of 26 dB and 37 dB, respectively. It is also observed that the multipactor behavior of the ferrite loaded waveguides remains very close to the without ferrite case for low frequency gap values (below 2.5 GHzmm). In general terms, the multipactor RF voltage threshold of the

ferrite loaded waveguide cases tends to be equal or below the without ferrite multipactor threshold.

In order to have a better understanding of the behavior of the different multipactor susceptibility curves, a detailed analysis of the RF electromagnetic fields (spatial distribution, scale analysis of the different electric and magnetic spatial components), and electron dynamics (resonant trajectories, multipactor order) has been performed for both the ferrite loaded waveguides and the classical unloaded (empty) metallic parallel-plate waveguide.

An exhaustive inspection of the RF electromagnetic field pattern of the three ferrite loaded waveguide cases has revealed that the RF magnetic field has very little influence in the electron motion, thus the contribution of the terms $v_i\, B_{RF,j}$ (being $i, j = x, y, z$) can be neglected in the differential equations of the electron motion. Regarding the RF electric field components, it has been found that all of them have noticeable effects in the electron trajectories. In Fig. 4 (left) it has been depicted the quotient between the maximum absolute value along the gap of $E_{RF,x}$ and $E_{RF,y}$ components for the different considered ferrite waveguides. In a similar way in Fig. 4 (right) it has been plotted the same quotient for the $E_{RF,z}$ and $E_{RF,y}$ components. From these figures it is extracted that the $E_{RF,y}$ is the greater RF electric field component for low frequency gap values. As the frequency gap increases the components $E_{RF,x}$ and $E_{RF,z}$ also grow with regard to the $E_{RF,y}$ component. This increment is found to be more notorious for the ferrite loaded waveguides with higher gaps. In fact, it can be observed that $E_{RF,x}$ becomes the dominant component in the $d = 2$ mm waveguide for values above 15 GHzmm.

Taking the previous statements into account, the differential equations of motion can be approximated in the following way for the earlier stages of the electron multiplication
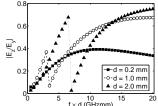
Fig. 4. Left (right): quotient between the maximum absolute value along the gap of the $E_{RF,x}$ ($E_{RF,z}$) and $E_{RF,y}$ components for the ferrite loaded waveguides.

$$\frac{dv_x}{dt} \simeq \omega_c v_z - \frac{e}{m} E_{RF,x} \cos(\omega t + \phi) \qquad (1)$$

$$\frac{dv_y}{dt} \simeq -\frac{e}{m} E_{RF,y} \cos(\omega t + \phi) \qquad (2)$$

$$\frac{dv_z}{dt} \simeq -\omega_c v_x - \frac{e}{m} E_{RF,z} \sin(\omega t + \phi) \qquad (3)$$

Here, $E_{RF,x}$, $E_{RF,y}$, $E_{RF,z}$ are the x, y, z RF electric field components, respectively, which only depend on the y coordinate; $\omega_c = \frac{e}{m} \mu_0 H_0$ is the cyclotron angular frequency, $\omega = 2\pi f$ is the RF angular frequency (f being the RF frequency), v_x, v_y, and v_z are the x, y, z components of the velocity vector, respectively; and ϕ is the phase of the RF electromagnetic field. It is remarkable that in such conditions the equation of motion for the y coordinate gets decoupled from the remaining x and z coordinates. Indeed, the approximated y-equation of motion becomes the corresponding one of the analytically well-studied classical case without ferrite [1], [2]. The effect of the external field H_0 is to spin the electron orbits in the xz plane. In addition, the $E_{RF,x}$ and $E_{RF,z}$ components accelerate the electron along the directions x and z, respectively. Manipulating the expressions (1) and (3) the following differential equations arise for the v_x and v_z velocities

$$\frac{d^2 v_x}{dt^2} + \omega_c^2 \, v_x = A_1 \, \sin(\omega t + \phi) \qquad (4)$$

$$\frac{d^2 v_z}{dt^2} + \omega_c^2 \, v_z = A_2 \, \cos(\omega t + \phi) \qquad (5)$$

where $A_1 = \frac{e}{m}(E_{RF,x,0}\,\omega - E_{RF,z,0}\,\omega_c)$ and $A_2 = \frac{e}{m}(E_{RF,x,0}\,\omega_c - E_{RF,z,0}\,\omega)$. The above differential equations can be solved analytically provided that the amplitude of the RF electric field components are uniform along the gap. Although this is not true in our case, we will take this assumption in order to obtain some analytical expressions that can give us a certain qualitative insight of the multipactor phenomenon. After some calculations, the following expressions arise for the v_x and v_z velocities (it is assumed zero initial velocity for

both coordinates)

$$v_x = \frac{A_1}{\omega_c^2 - \omega^2} \sin(\omega t + \phi) - \frac{A_1 \, \sin(\phi)}{\omega_c^2 - \omega^2} \cos(\omega_c t)$$

$$-\frac{A_2 \, \cos(\phi)}{\omega_c^2 - \omega^2} \sin(\omega_c t) \qquad (6)$$

$$v_z = \frac{A_2}{\omega_c^2 - \omega^2} \cos(\omega t + \phi) - \frac{A_2 \, \cos(\phi)}{\omega_c^2 - \omega^2} \cos(\omega_c t)$$

$$+\frac{A_1 \, \sin(\phi)}{\omega_c^2 - \omega^2} \sin(\omega_c t) \qquad (7)$$

Note that (6) and (7) are valid for all the RF frequencies except for $\omega = \omega_c$. For both velocities there are oscillatory terms at both the RF frequency and at the cyclotron frequency. It is easily noticed that the amplitude of these oscillations becomes maximum when the RF frequency equals the cyclotron one ($\omega = \omega_c$). Consequently, the velocity gain in the plane xz is maximum in the neighborhood of such resonance. In our case the cyclotron frequency is 8.4 GHz and the corresponding frequency gap is 8.4 GHzmm for the $d = 1$ mm waveguide and 16.8 GHzmm for the $d = 2$ mm waveguide. This cyclotron resonance allows to understand the sharp minimums observed for the multipactor RF voltage thresholds of the ferrite loaded waveguides with $d = 1$ mm and $d = 2$ mm in the surroundings of such frequency gap values. Due to the enhance in kinetic energy gain of the electron in the xz plane, less RF voltage amplitude is necessary to achieve that the total kinetic impact energy of the electron exceeds the W_1 of the material. To illustrate the cyclotron resonance effect, in Fig. 5 we have plotted the v_x, v_y, v_z velocities of an effective electron in the $d = 1$ mm ferrite loaded waveguide, for a frequency gap value close to the resonance and an RF voltage value corresponding to the multipactor threshold. It is noticed the increment of the v_x and v_z maximum amplitude in the successive oscillations between one impact and next, whilst for the v_y velocity it is not observed such maximum amplitude increment. In Fig. 5 it has also been depicted the xz-plane electron trajectory which seems very similar to that of a cyclotron accelerator, where the radius of the electron circular trajectory tends to increase as the kinetic energy gain process is ongoing.

The above statements justify the presence of a sharp minimum in the multipactor RF voltage threshold for the frequency gap values in the vicinity of the cyclotron resonances for the $d = 1$ mm and $d = 2$ mm ferrite loaded waveguide cases. However, it is notorious that such multipactor RF voltage threshold minimum is not observed for the $d = 0.2$ mm waveguide (which should be expected at 1.68 GHzmm). To understand this point we will briefly recall some aspects of the classic multipactor theory for parallel-plate waveguides. As it is well known, for the onset of a multipactor discharge it is required that the electron becomes synchronized with the RF electric field (it implies the apparition of stable resonant trajectories, also known as multipactor modes), and an electron impact kinetic energy with the waveguide walls above the W_1 parameter of the material (which ensures the release of secondary electrons). The classical multipactor modes that guarantee the electron synchronization with the RF electric field consist on electron trajectories that take an odd number
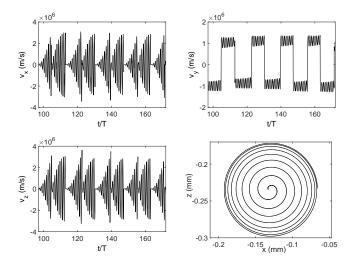
Fig. 5. From left to right, and up to down: effective electron velocity components as a function of the time normalized to the RF period (T is the RF period), and xz-plane electron trajectory. All for a ferrite waveguide with $d = 1$ mm, $f \times d = 8.5$ GHzmm, $V_0 = 25$ V.

of RF semiperiods to cross the gap (the multipactor order N is defined as that number of RF semiperiods).

In our ferrite loaded waveguide case, we have argued previously that the y motion becomes decoupled from the x and z coordinates, resulting in the same y differential equation of motion that for the classical metallic parallel-plate waveguide. The only difference in the y equation of motion between the unloaded ferrite waveguide and the ferrite waveguide is that, in the latter case, the $E_{RF,y}$ is inhomogeneous along the gap. However, we can take the assumption of spatial homogeneity as a first approach to our problem. When such consideration is done, we can use the classical multipactor modes and formulas to qualitatively explain the ferrite loaded waveguide. We will rely on two expressions to reach this aim. The first expression, $V_{0,min}$, gives the minimum RF voltage that guarantees a resonant multipactor of order N. To deduce such equation we have imposed that an electron starting from $y = 0$ arrives to $y = d$ in a time $\frac{NT}{2}$, then we have searched the starting phase of the RF field (ϕ) that gives the lowest RF value [1], [2]:

$$V_{0,min} = \frac{m}{e} \frac{(\omega d)(\omega d - v_{0y}\pi N)}{2\sqrt{1 + \left(\frac{\pi N}{2}\right)^2}} \qquad (8)$$

where v_{0y} is the y-component of the initial velocity. It must be remarked that the RF voltage calculated with (8) does not ensure that the kinetic energy due to v_y is above the W_1 parameter. The second expression is for the RF voltage that ensures a resonant multipactor mode of order N with an electron impacting with a kinetic energy of W_1, i.e., V_{0,W_1}. In some cases the values given by expressions of V_{0,W_1}. or $V_{0,min}$ may not correspond to valid resonant trajectories. The procedure to deduce V_{0,W_1} consists of imposing the two aforementioned conditions in the equations of the y trajectory
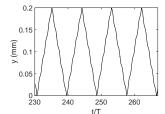
and the v_y velocity. Finally it is obtained that

$$V_{0,W_1} = \frac{m}{e} \frac{(\omega d)(\omega d - v_{0y}\pi N)}{\pi N \sin \phi_{W_1} - 2 \cos \phi_{W_1}} \qquad (9)$$

$$\phi_{W_1} = arc \cot \left(\frac{\pi N}{2} - \frac{\omega d - v_{0y}\pi N}{v_{iy}} \right)$$

where v_{iy} is the y impacting velocity that is set to match with the W_1 kinetic energy. Note that expressions (8) and (9) depend on the frequency gap product. For each frequency gap value, it can be estimated the minimum RF voltage at which each of the multipactor modes appears.

The first multipactor modes at a frequency gap value of 8.4 GHzmm are shown in Table I. The first column indicates the order of the multipactor mode N; second column gives the RF voltage to ensure the resonant electron impacts with a kinetic energy equal to the W_1 (19 eV in our case) of the material, V_{0,W_1}; third column provides the minimum RF voltage at which the resonant trajectories appear, $V_{0,min}$; and fourth column is for the electron impact kinetic energy when the RF voltage is $V_{0,min}$, $W_{i,V_{0,min}}$. If $W_{i,V_{0,min}}$ is equal or above W_1 then $V_{0,min}$ is the multipactor RF voltage threshold for the N mode, if not the multipactor RF voltage threshold is $V_{0,W1}$. At the view of the results summarized in Table I, the $N = 9$ multipactor mode appears at an RF voltage threshold lower than the other available modes ($N = 1, 3, 5, 7$), which appear at higher RF voltages than the multipactor threshold. Electron resonant trajectories with $N = 11, 13, 15, ...$ may appear but cannot contribute to the eventual onset of the discharge since their impacting energies are below W_1. The results of the multipactor numerical simulations for the without ferrite waveguide are in concordance with the theoretical predictions of Table I. Indeed, in Fig. 6 (left) it is depicted the effective electron vertical trajectory at 8.4 GHzmm in the multipactor RF voltage threshold, revealing the presence of a resonant multipactor with $N = 9$. In Fig. 6 (right) it is depicted the effective electron vertical trajectories at the same frequency gap in the multipactor RF voltage threshold for the ferrite loaded waveguide with $d = 1$ mm. Note that at this frequency gap, the cyclotron resonance occurs and the multipactor RF voltage threshold is clearly below the without ferrite value. For this case, it cannot be found a well-defined multipactor order, instead a hybrid multipactor than ranges from order 15 to 19 appears (see Fig. 6 (right)). According to Table I, for such multipactor modes, there are no RF voltages that give an impact kinetic energy of the electron equal or above the W_1 of the material. Although resonant trajectories can appear (when the RF voltage exceeds $V_{0,min}$), their impacting energies are quite below the W_1 (5.4 eV and 3.5 eV for the multipactor orders 17 and 19, respectively). However, these impacting energies have been obtained for the classical metallic paralel-plate waveguide (without ferrite), where there is only vertical RF electric field that accelerates the electron along that spatial direction. In the ferrite loaded case, the RF electric fields in the tranverse xz-plane induce an acceleration which is uncoupled from the vertical dynamics of the electron but contributes to its total kinetic energy. Indeed, after analyzing the different spatial contributions to the electron total kinetic energy, it is noticed that the xz-plane contribution notoriously exceeds the
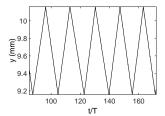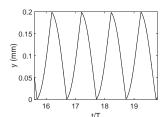
Fig. 6. Vertical coordinate effective electron trajectories as a function of the time normalized to the RF period, $f \times d = 8.4$ GHzmm. Left: metallic parallel-plate waveguide (without ferrite case), $V_0 = 518$ V. Right: ferrite loaded waveguide with $d = 1$ mm, $V_0 = 25$ V.
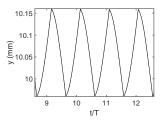

Fig. 7. Vertical coordinate effective electron trajectories as a function of the time normalized to the RF period, $f \times d = 1.68$ GHzmm. Left: metallic parallel-plate waveguide (without ferrite case), $V_0 = 104$ V. Right: ferrite loaded waveguide with $d = 0.2$ mm, $V_0 = 103$ V.

vertical contribution (recall Fig. 5). This occurs because the xz-plane acceleration is maximum at the frequency gap value that fits the cyclotron resonance. This fact allows to reduce the multipator RF voltage threshold in the ferrite case with regard to the without ferrite case, thus moving from a multipactor order 9 (without ferrite case) to a 17-19 multipactor order (ferrite case).

Table I
Multipactor modes for $f \times d = 8.4$ GHzmm.

N	V_{0,W_1} (V)	$V_{0,min}$ (V)	$W_{i,V_{0,min}}$ (eV)
1	7111	4043	1579
3	5487	1390	280
5	3864	743	95
7	2244	459	43
9	656	300	23
11	x	199	14
13	x	129	8.4
15	x	77	5.4
17	x	37	3.5
19	x	6	2.3

In the same way that for Table I, the first resonant modes for $f \times d = 1.68$ GHzmm are shown in Table II. At this frequency gap value only the multipactor mode with $N = 1$ can contribute to the multipactor discharge in the unloaded ferrite waveguide. Resonant trajectories with orders 3 and 5 may exist, but their impacting energies are insufficient to release secondary electrons. In Fig. 7 (left) it is depicted the effective electron vertical trajectory at 1.68 GHzmm in the multipactor RF voltage threshold for the without ferrite case; it can be observed the presence of the predicted multipactor mode of order 1. In Fig. 7 (right) it is also shown the effective electron vertical trajectory at the same frequency gap value for the ferrite waveguide with $d = 0.2$ mm; it is noticed the presence of the same multipactor mode ($N = 1$) that in the without ferrite case. Although for the ferrite case the frequency gap value matches the cyclotron resonance, the other available multipactor modes ($N = 3$ and $N = 5$) have too short flight time between successive impacts with the device walls, preventing the energy gain in the xz-plane due to the cyclotron resonance. This fact justifies that the multipactor RF voltage thresholds are equal in the loaded and unloaded ferrite cases.

Table II
Multipactor modes for $f \times d = 1.68$ GHzmm.

N	V_{0,W_1} (V)	$V_{0,min}$ (V)	$W_{i,V_{0,min}}$ (eV)
1	162	126	55
3	x	15	5.2
5	x	11	0.7

As it is well stated in the classical multipactor theory, the number of multipactor modes available for a multipactor discharge grows as the frequency gap increases [2]. In the same way, the flight time between successive electron impacts rises up as the multipactor order does. Thus, low frequency gap values imply low crossing gap times for the electrons. This fact justifies similarity in the multipactor RF voltage threshold between the ferrite waveguide and the without ferrite cases for the low frequency gap values (remember Fig. 3). Despite the presence of the accelerating RF electric field in the xz-plane, the contribution to the electron kinetic energy is quite low due to short transit time. However, when the frequency gap increases the flight time also does, allowing higher gain in the transverse plane kinetic energy, and so reducing the multipactor RF voltage threshold regarding the without ferrite case (recall Fig. 3).

Previously we have analyzed ferrite waveguides with vacuum gaps of 0.2 mm, 1.0 mm and 2.0 mm, and a total height equal to the standard WR-90 waveguide. For completeness, we try a ferrite loaded waveguide with a gap of $d = 5$ mm. According to the above statements, for the frequency gap value that matches the cyclotron resonance (in this case 42 GHzmm), it is expected a sharp minimum in the multipactor RF voltage threshold. Indeed, the results from the numerical simulations for the multipactor RF voltage threshold in the $d = 5$ mm ferrite waveguide shown in Fig. 8 confirm this statement. It should be remarked that for a classical metallic parallel-plate waveguide, no multipactor discharge is expected at such high frequency gap values at the RF voltage levels employed in the RF satellite telecommunication systems.

Finally, it has been analyzed the case of having different SEY coefficients for the ferrite and the metal surface. The SEY parameters for the ferrite remain the same that were described previously in this section, whilst the SEY coefficients for the metal are those from the ECSS silver [3], i.e., $W_1 = 30$ eV, $W_{max} = 165$ eV, and $\delta_{max} = 2.22$. In Fig. 9 it is shown the multipactor RF voltage threshold for the ferrite waveguide with $d = 0.2$ mm considering the ferrite and silver SEY
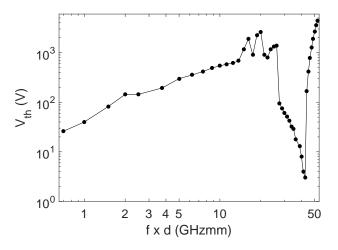
Fig. 8. Multipactor RF voltage threshold as a function of the frequency gap for a ferrite waveguide with $d = 5$ mm and $b = 10.16$ mm.
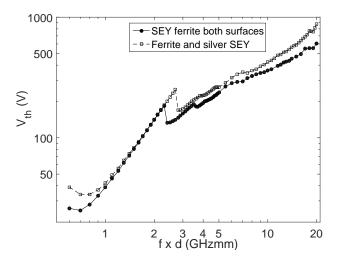

Fig. 9. Multipactor RF voltage threshold as a function of the frequency gap for a ferrite waveguide with $d = 0.2$ mm and $b = 10.16$ mm, considering the same SEY properties for both surfaces and considering different SEY for ferrite and metal (silver) surfaces.

properties, as well as the results considering the same SEY properties for both surfaces. It is observed slight differences between both cases. Note that the multipactor RF voltage threshold in the ferrite and silver SEY case tends to be greater than in the case with the same SEY in both surfaces, this is because the W_1 for silver is above the W_1 for the ferrite, and more RF voltage amplitude is required in the former case to reach the multipactor threshold.

IV. CONCLUSIONS

In this paper, the multipactor effect in a parallel-plate waveguide containing a magnetized ferrite slab has been studied. In order to magnetize the ferrite, an external static magnetic field oriented along the vertical direction was assumed. A home-made 3D code based on the effective electron model was developed to carry out numerical simulations that allowed to compute the multipactor RF voltage threshold. The multipactor susceptibility charts obtained show that the multipactor RF

voltage threshold changes with regard to the classical metallic parallel-plate situation with neither ferrite slab nor external magnetic field. In fact, a considerable reduction threshold with respect to the classic parallel-plate case has been found at some frequency gap ranges. Moreover, the analysis of the effective electron trajectories has led to a better understanding of the multipacting phenomenon in waveguides loaded with magnetized ferrites.

REFERENCES

[1] J. Vaughan, "Multipactor", *IEEE Trans. Electron Devices*, Vol. 35, No. 7, pp. 1172-1180, July 1988.
[2] A.J. Hatch, H.B. Williams, "Multipacting Modes of High-Frequency Gaseous Breakdown", *The Physical Review*, vol. 112, no. 3, pp. 681-685, Nov. 1958.
[3] "Multipaction design and test", ECSS-E-20-01A, ESA-ESTEC, 2003.
[4] A. M. Pérez, C. Tienda, C. Vicente, S. Anza, J. Gil, B. Gimeno, V. E. Boria, "Prediction of Multipactor Breakdown Thresholds in Coaxial Transmission Lines for Traveling, Standing, and Mixed Waves", *IEEE Trans. Plasma Science*, Vol. 37, no. 10, Oct. 2009.
[5] V. E. Semenov, E. I. Rakova, D. Anderson, M. Lisak, J. Puech, "Multipactor in rectangular waveguides", *Physics of Plasmas*, vol. 14, 033501, 2007.
[6] V. E. Semenov, N. A. Zharova, D. Anderson, M. Lisak, J. Puech, "Simulations of multipactor in circular waveguides", *Physics of Plasmas*, vol. 17, 123503, 2010.
[7] A. Coves, G. Torregrosa-Penalva, C. Vicente, B. Gimeno, and V. E. Boria, "Multipactor discharges in parallel-plate dielectric-loaded waveguides including space-charge effects", *IEEE Trans. on Electron Devices* vol. 55, no. 9, pp. 2505-2511, Sep. 2008.
[8] L. K. Ang, Y. Y. Lau, R. A. Kishek and M. Gilgenbach, "Power deposited on a dielectric by multipactor", *IEEE Trans. on Plasma Science* vol. 26, no. 3, pp. 290-295, June 1998.
[9] R. A. Kishek, Y. Y. Lau, L. K. Ang, A. Valfells, and R. M. Gilgenbach, "Multipactor discharge on metals and dielectrics: Historical review and recent theories", *Physics of Plasmas*, Vol. 5, no. 5, May 1998.
[10] V. E. Semenov, E. Rakova, M. Belhaj, J. Puech, M. Lisak, J. Rasch, E. Laroche, "Preliminary results on the Multipactor effect prediction in RF components with ferrites", *Vacuum Electronics Conference (IVEC), 21-23 May 2013, Paris, IEEE 14th International.*
[11] D. González-Iglesias, B. Gimeno. V. E. Boria, Á. Gómez, A. Vegas "Multipactor Effect in a Parallel-Plate Waveguide Partially Filled With Magnetized Ferrite", *IEEE Trans. on Electron Devices* vol. 61, no. 7, pp. 2552-2557, July 2014.
[12] R.L. Geng, H. Padamsee, S. Belomestnykh, P. Goudket, D.M. Dykes, R.G. Carter, "Suppression of multipacting in rectangular coupler waveguides", *Nuclear Instrum. Methods Physics Res. A*, Vol. 508, pp. 227-238, 2003.
[13] V. E. Semenov, N. A. Zharova, N. I. Zaitsev, A. K. Gvozdev, A. A. Sorokin, M. Lisak, J. Rasch, J. Puech, "Reduction of the Multipactor Threshold Due to Electron Cyclotron Resonance", *IEEE Transactions on Plasma Science*, vol. 40, no. 11, pp.3062-3069, Nov. 2012.
[14] David M. Pozar, "Microwave Engineering", 4th edition, *John Wiley & Sons, Inc.*, 2012.
[15] A. J. Baden Fuller, "Ferrites at Microwave Frequencies", IET Electromagnetic Wave Series no. 23, *The Institution of Enginering and Technology*, 2008.
[16] J. Helszajn, "Waveguide Junction Circulators Theory and Practice", *John Wiley & Sons*, 1998.
[17] Robert E. Collin "Foundations for Microwave Engineering", Second Edition, *McGraw-Hill, Inc.*, 1992.

[18] S. Anza, C. Vicente, D. Raboso, J. Gil, B. Gimeno, V. E. Boria, "Enhanced Prediction of Multipaction Breakdown in Passive Waveguide Components including Space Charge Effects", *Microwave Symp. Digest, 2008 IEEE MTT-S*, pp. 1095-1098.

[19] J.R.M. Vaughan, "Secondary Emission Formulas", *IEEE Trans. Electron Devices*, Vol. 40, no. 4, pp. 830, April 1993.

[20] J. Greenwood "The correct and incorrect generation of a cosine distribution of scattered particles for Monte-Carlo modelling of vacuum systems", *Vacuum*, vol. 67, no. 2, pp. 217-222, September 2002.

[21] S.A Schelkunoff, "Generalized telegraphist's equations for waveguides", *Bell Syst. Tech. J.*, vol. 3, no. 4, pp. 784-801, July 1952.

[22] Á. Gómez, J. S. Ipiña, M. A. Solano, A. Prieto, A. Vegas, "Improving the coupled-mode method by means of step functions: Application to partial-height isotropic or anisotropic dielectric parallel-plate waveguides", *Microw. Opt. Techn. Lett.*, vol. 33, no. 6, pp. 408-414, June 2002.

[23] Á. Gómez, A. Lakhtakia, A. Vegas, M. A. Solano, "Hybrid technique for analysing metallic waveguides containing isotropic chiral materials", *IET Microw., Antennas Propag.*, vol. 4, no. 3, pp. 305-315, Mar. 2010.

[24] I. Montero, F. Caspers, L. Aguilera, L. Galán, D. Raboso, and E. Montesinos, "Low-Secondary Electron Yield of Ferromagnetic Materials and Magnetized Surfaces", *Proc. IPAC'10*, Kyoto, Japan, 23-28 May, 2010.